Physics based data driven method for the crashworthiness design of origami composite tubes

Int J Mech Mater Des
https://doi.org/10.1007/s10999-023-09685-2

Physics based data driven method for the crashworthiness design of origami composite tubes

Alberto Ciampaglia · Dario Fiumarella · Carlo Boursier Niutta · Raffaele Ciardiello · Giovanni Belingardi

Received: 20 July 2023 / Accepted: 22 September 2023

Abstract A novel method based on a physics informed data driven model is developed to design an origami composite crash tube. The structure consists of two axially stacked basic components, called modules. Each module presents lower and upper square sections with an octagonal section in the middle. The parameters of the octagonal cross-section and the height of each module are optimized to maximize the energy absorption of the tube when subjected to an axial impact. In contrast to standard surrogate modelling techniques, whose accuracy only depends on the amount of available data, a Physics-informed Neural Network (PINN) scheme is adopted to correlate the crushing response of the single modules to that of the whole origami tube, constraining the data driven method to physically consistent predictions. The PINN is first trained on the results obtained with an experimentally validated Finite Element model and then used to optimize the structure. Results show that the PINN can accurately predict the crushing response of the origami tube, while consistently reducing the computational effort required to explore the whole design domain. Also, the comparison with a standard Feed Forward Neural Network (FFNN) shows that the PINN scheme leads to more accurate results.

Keywords Carbon fibre · Vehicle · Machine learning · Optimization · Energy absorption

1 Introduction

The safety requirements for vehicle crashes are escalating due to several factors. Firstly, there is a growing emphasis on reducing the risk of occupant injury and fatalities in accidents. Additionally, stricter regulations are being implemented to ensure vehicles meet higher safety standards. The latest regulations from the NCAP have set higher safety requirements for the vehicles, increasing the speed in most of the critical tests and introducing additional crash tests for the assessment of overall vehicle safety. From the engineering perspective, the effective enhancement of the body's structural performance in crash scenarios necessitates the integration of multiple factors, and conventional optimization methods reach their limitations when tackling this issue. Furthermore, due to the profoundly non-linear nature of crashes, discovering a crash structure configuration that achieves optimal behaviour (efficiently absorbing substantial energy, minimizing weight, and adhering to manufacturing limitations) is exceptionally intricate. Consequently, the design procedure remains predominantly manually driven, relying heavily on the expertise and

A. Ciampaglia (✉) · D. Fiumarella · C. Boursier Niutta · R. Ciardiello · G. Belingardi
Department of Mechanical and Aerospace Engineering, Politecnico di Torino, C.so Duca degli Abruzzi 24, Turin, Italy
e-mail: alberto.ciampaglia@polito.it

Published online: 16 October 2023

accumulated knowledge of engineers developed over time. Novel methodologies that can leverage the engineering knowledge of the crash mechanism, while reducing the design time, are then necessary to accelerate the design of these structures and efficiently target the safety requirements.

Crash boxes are sacrificial components which aim at absorbing the kinetic energy during low-velocity impact events through mechanical deformation, thus limiting injuries to the occupants, and preserving the structural integrity of the rest of the front car body, of the components in the engine compartment and the vehicle suspension system. To reach the goal of low-weight yet safe structures, composite materials are increasingly adopted in the design of automotive parts as crash absorbers, given their superior specific mechanical performances compared to metals (Ciampaglia et al. 2020a; Koronis et al. 2013; Martulli et al. 2020; Rwawiire et al. 2015). Several studies and applications of composite materials in crash tubes are reported in the literature, showing the good mechanical performances in crash absorbers (Boria et al. 2015, 2016, 2019).

Among the different design solutions, pre-folded origami tubes have shown a consistent reduction of the peak force and comparable energy absorption capabilities (Ma & You 2014) if compared with conventional geometries, which results in reduced acceleration to vehicle passengers and improved safety. (Zhao et al. 2011) proposed a geometrical optimization of cylindrical origami tubes to enhance the energy absorption capability. Similar works (Boreanaz et al. 2020; Li & You 2019; Ye et al. 2019; Zhou et al. 2017) on different origami pattern tubes have demonstrated the benefits and the wide domain of solutions achievable with these structures. More recently, (Wu et al. 2022) have proposed a design strategy to avoid unstable global bending in the axial crash. They showed that the crush response of specifically designed origami tubes followed the deformation of the crease, thus avoiding global bending. (Ye et al. 2020) have shown that the brittle failure of hybrid tubes made of carbon fibre and Kevlar fibre-reinforced plastics, which is difficult to predict and can lead to inefficient use of the material, can be prevented through origami patterns. For a comprehensive and recent review of the topic, the reader can refer to the work of (Ma et al. 2022).

The main advantage of origami patterns is that a change in the geometrical parameters of such structure does not affect the mass of the component, differently from the standard squared, tapered or cylindrical geometries. Thus, the geometrical parameters can be tuned to maximize the crushing performance of the structure while keeping a target mass. Further, pre-folded tubes can be designed to achieve stable and progressive crushing mode.

1.1 Motivation

Structural optimization assists in designing crashworthy and lightweight structures. However, given the high influence of the shape on the collapsing mode and the absorbed energy, especially in the case of composite materials, the identification of the optimal configuration is challenging in crashworthiness design problems, which are generally ill-posed (Baler 1994; Hadamard 1902). A large amount of data, both experimental and numerical, is required to assess the influence of the tube shape on its crushing response. To reduce the computational time, while gaining information on the whole design domain, previous research has increasingly adopted surrogate modelling techniques, especially in crashworthiness problems (Avalle et al., n.d.; Fiumarella & Raponi 2020; Hou et al. 2007; Raponi et al. 2021). Modified approaches have been also proposed, which aim at reducing the design domain at each iteration of the optimization problem or at increasing the accuracy by sampling in the proximity of an optimal configuration (Dias et al. 2005; Hou et al. 2007). Even though the design domain can be widely investigated through surrogate models, limitations are still present, as the accuracy of the interpolation strongly depends on the amount of available data.

Recent works have proposed machine learning based techniques to model the effect of the geometry of crash structures on their response: (Sakaridis et al. 2022) developed a machine learning model to predict the crash response of tubular structures using a standard Neural Network (NN), while (Zhang et al. 2022) used a clustering algorithm to identify three characteristic collapsing mode of the origami structures to correlate these with the tube geometry.

1.2 Aim of the work

This research aims at providing an efficient and reliable methodology for designing the collapse response of crush tubes made of composite materials. The core focus is on leveraging Physics-informed Neural Networks (PINN) to predict the crush response of the origami-shape crush tubes accurately and enhance the design process for crashworthy components. Traditional methods, relying on computationally intensive simulations and large datasets, often face limitations in terms of accuracy and efficiency. Indeed, conventional optimizations based on surrogate models demand extensive computational resources, abundant datasets composed by time-consuming simulations to achieve acceptable accuracy, which can hinder the design process. The idea underlying PINN, firstly proposed by (Raissi et al. 2019), is to train NN by minimizing a loss function that contains both a prediction error and a physics regularization error, thus ensuring the physics compliance of the prediction. The employment of PINN thus aims to streamline the design cycle, making it more feasible to explore a wide design domain while maintaining high prediction accuracy and offering an improved solution for complex crashworthiness design.

The central aspect lies in the prediction of the energy absorption characteristics and to optimize the geometric parameters of origami-shaped crash tubes, striving to maximize energy absorption while minimizing peak forces, which could affect occupant safety. In this regard, it is worth mentioning that, recently, novel physic-based machine learning models have been proposed that adopt an energy approach to solve mechanical problems with machine learning methods (Samaniego et al. 2020).

The origami structure here retained consists of two axially stacked basic structures, called modules, each presenting a lower and upper square section and an octagonal section in the middle and is made of two carbon fibre woven fabric plies. The PINN aims at correlating the crushing response of the single modules to that of the whole origami tube. A shape parameter of the octagonal cross section and the height of the module are varied through a morphing strategy and following a Latin Hypercube (LH) DoE scheme. Finite Element (FE) analyses of the single modules and the corresponding whole tubes are performed in the LS-Dyna environment to train the network. The FE model was at first validated by comparing numerical simulation results with the experimental results of the crushing tests on a single module structure. The proposed scheme allows for the investigation of a large design domain with consistently reduced computational effort. The PINN is then used to optimize the crushing performance of the structure. Two optimal configurations are identified by the PINN with similar performance. The predicted absorbed energy and its trend with the proceeding of the collapse displacement are compared with FE analyses. Results show a good agreement, thus proving the effectiveness of the devised methodology. Finally, the comparison of the results obtained with a standard FFNN shows that the PINN scheme leads to more accurate results.

2 Materials and methods

Firstly, the carbon fibre woven fabric used in the crash tubes is presented. Then the considered origami geometry and the adopted FE model are described. The FE model was previously validated by comparison with the experimental characterization of the crash response of the single module. Then, the shape morphing methodology adopted to generate the numerical Design of Experiments (DoE) according to a Latin Hypercube sampling scheme is presented. FE analyses are performed to train both the PINN and the FFNN. The loss functions of the two networks are finally detailed at the end of the section.

2.1 Materials

Carbon fibre woven fabric pre-impregnated with epoxy resin, named XPREG XC130, is considered for the origami tube. Tensile, compressive and shear properties have been assessed in our previous work (Ciampaglia et al. 2020a, b) through a servo-hydraulic machine Instron 8801 and in accordance with the specifications of the Standards ASTM D3039, ASTM D3410 and ASTM D5379 (ASTM International, n.d.; International 2011; Nemeth, n.d.). Table 1 reports the mean values and the standard deviations at the lamina level resulting from three repetitions of each test.

Table 1 also reports the ultimate stresses and ultimate strains, necessary for the complete

Table 1 Material properties of the XPREG XC110

Property	Mean value	STD
Density [kg/m^3]	1450	–
In-plane Poisson's ratio	0.12	–
Longitudinal modulus [MPa]	58,000	340
Transverse modulus [MPa]	58,000	340
Longitudinal tensile strength [MPa]	440	16
Longitudinal tensile ultimate strain	0.0072	–
Longitudinal compressive strength [MPa]	453	36
Longitudinal compressive ultimate strain	0.096	–-
Transverse tensile strength [MPa]	440	16
Transverse compressive strength [MPa]	453	36
In-plane shear modulus [MPa]	3900	–
In-plane shear strength [MPa]	72	–

characterization of the material card. The thickness of the lamina is equal to 0.45 mm.

2.2 Geometry description

The basic principle of an origami structure is to fold a flat rectangular sheet and transform it into a three-dimensional shape. Figure 1 shows the origami geometry considered in this study in its unfolded and folded configurations. The image reports a single module of the full crash box, i.e., the basic structure that is then axially stacked to create the full crash tube. In the unfolded configuration, the sheet presents a rectangular shape with a major edge of 8*e* in length and a height equal to *l*. In its folded configuration, the origami tube presents an upper and lower square perimeter with a length equal to 8e, and an octagonal central perimeter with a total length of 8b + 4c. The unfolded configuration must have a rectangular shape; therefore, it holds that:

$$8b + 4c = 8e \tag{1}$$

The c value is the width of the rhomboidal lobe. The normal distance between the upper and the bottom rectangular perimeter (or the normal distance between the two vertexes of the rhomboidal lobe) is the height of the single module (*h* distance). Note that h is different from *l*, as in the folded configuration the origami faces are bent at an angle ϑ respect to the plane orthogonal to the tube axis.

2.3 Finite element model and experimental validation

The crushing response of the origami structure is assessed through transient nonlinear FE analyses in the LS-Dyna environment. The origami tube is modelled through Belytschko-Tsay 4 nodes shell elements with six degrees of freedom per node. This shell element formulation is based on the Reissner–Mindlin shell theory and accordingly allows to account for the shear deformations. Furthermore, the formulation implemented in LS-Dyna is even faster than standard Hughes-Liu shell elements, based on the Kirchoff-Love shell theory (Hallquist 2006). Therefore, the Belytschko-Tsay has been preferred for the explicit calculations of this work. After the convergence study, a mesh size of 5 mm is considered. The structure is composed of two layers of the carbon fibre woven fabric described in Sect. 2.1 and has a uniform thickness of 0.9 mm. The stacking sequence is specified through the *PART_COMPOSITE keyword, which assumes one integration point for each

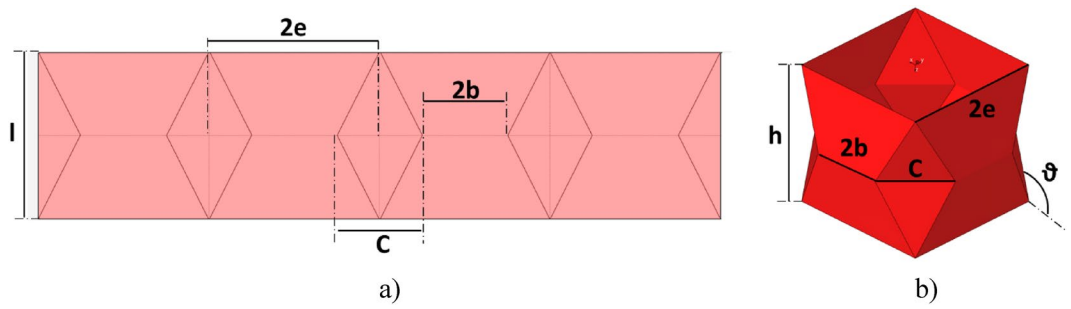

Fig. 1 Description of the origami single module geometry: **a** unfolded sheet; **b** folded single module origami structure

layer of the laminate. The anchorage of the crash-box structure to the vehicle frame is simulated by fully constraining the bottom nodes, while a rigid wall impacts the structure with an initial kinetic energy of 1.2 kJ with an impact speed of 2.5 m/s. This energy level guarantees the complete crush of the tube. The same conditions apply to the single module and full origami structure. The material under study presents a low sensitivity to the strain rate, thus its effect has not been modelled in the FEM.

The material is modelled with the material card *MAT_ENHANCED_COMPOSITE_DAMAGE (*MAT54/55), according to the properties reported in Table 1. The non-physical SOFT parameter was identified in the previous work (Ciampaglia et al. 2020a, b) by comparison with the compressive test of a single module. This parameter reduces the stiffness of the crush-front elements, thus simulating damage propagation and reducing the load oscillations. Figure 2a and b show the tested module and the corresponding FE model.

For further details, the reader is referred to (Ciampaglia et al. 2020a).

2.4 Machine learning methods

The machine learning framework presented in this work correlates the axial crushing response of the individual modules with the global response of the origami crash tube, obtained by vertically stacking the individual modules. This method assumes that the response of the single submodules is related to the response of the crash tube and finds a relation between those using a NN. The framework is visually described in Fig. 3.

The dataset generation, feature extraction, data preparation and the NN used in this work are described in the following paragraphs.

2.4.1 *Design of experiments (DoE)*

A set of numerical simulations of axial crushing of a single module structure with different lobe widths and heights (respectively named c and h, Fig. 1) is performed. The absorbed energy and force response is stored in a database and used as input to the machine learning algorithms. The design space of the single modulus geometry is described by the two variables, i.e., c and h, sampled within a range from 35 to 55 *mm* and 78 to 98 *mm*, respectively. A Latin Hypercube (LH) algorithm sampled 40 data points in the defined design space, yielding 40 different single-module geometries.

The DoE exploration is carried out by interfacing the geometric pre-processor Hypermorph with the software LS-Opt. The parameterization of the shape variables c and h is carried out through the Hypermorph software.

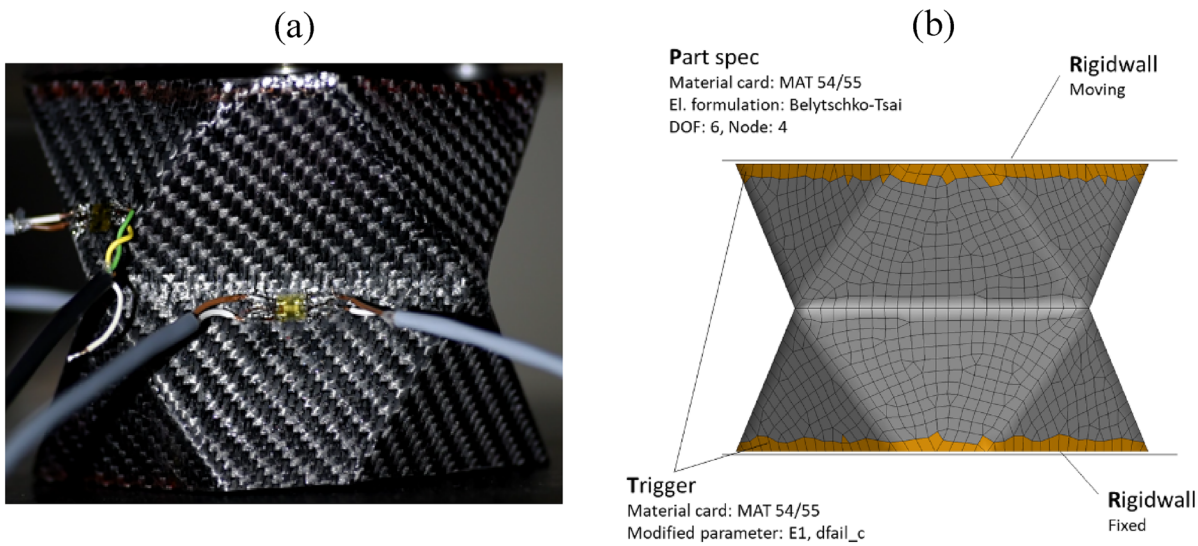

Fig. 2 Crushing test of a single module: **a** experimental setup; **b** numerical model

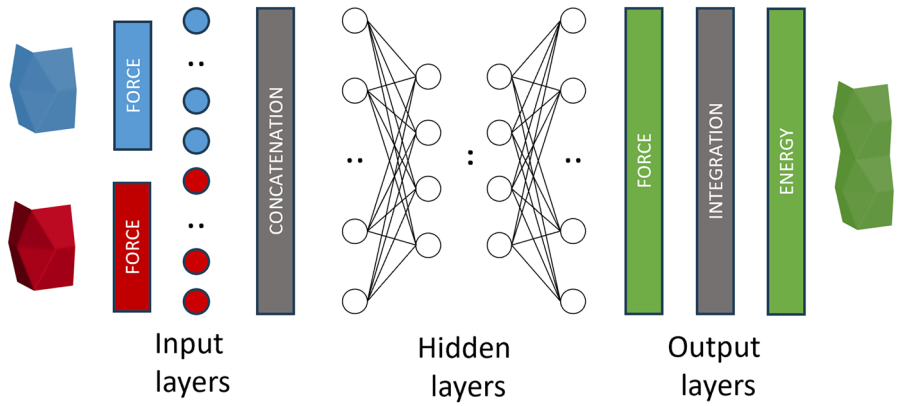

Fig. 3 Machine learning framework for the prediction of the crash tube response from the individual crash of the sub-modules

The parameters are passed to a morphing script that modifies the single modulus mesh by preserving:

- The planarity of the crash tube edges;
- The total area of the mid-surface, complying with the definition of an origami-inspired thin-walled structure;
- The total number of elements in the mesh.

As the origami crash tube presents two cross-sectional symmetry planes, only a quarter of the module is modelled (Fig. 4a).

The different geometry shapes are generated without a remeshing algorithm: the morphing of the structure deforms and stretches the mesh elements to an accepthat the output of the last layertable extent and without worsening the mesh quality indices. The generation of the morphed shapes is divided into two steps: morphing of the module height h and morphing of the lobe width c.

The *x,y* and *z* degrees of freedom (DOF) of the nodes belonging to the edge *e* are constrained to node 1 (Fig. 4).

Accordingly, when node 1 is moved along the z direction, the module is morphed in its height. A plane passing through the *b* edge and parallel to the *xy* plane is created to guarantee a symmetric morphing relation and equally stretches the two-half portions of the module. As the morphing of the structure requires preserving the planarity of the crash box edges (i.e., Eq. (1) must hold), the variation of the *c* parameter requires particular attention. The translational DOFs along the *x* and *y* directions of the nodes belonging respectively to the right and left vertical free edges (edges 1 in Fig. 4b) are constrained. Consequently, the *b* edges can only rigidly translate orthogonally to their direction, i.e., along the *v* arrow in Fig. 4b. The nodes of edge *b* are constrained to move only along the *k* direction. Accordingly, when the *c* value is increased, the *c* edge nodes move in the *u* direction, and the *b* edge elements shorten along *k*. Also, the *b* edges move along *v,* and the angle between the module faces decreases. Figure 4b shows two examples of geometrical morphing applied to the origami module. As can be noticed from the configuration C-10/h + 10, as the *c* value decreases, the angle between the faces increases. Ideally, if *c* is reduced to 0, the origami module morphs into a square-section parallelepiped.

Once defined the input database, we computed the 1560 possible double module geometries from single module combinations and sampled a subset of 100 configurations (shown in Fig. 5). These 100 double module configurations have been sampled through a discrete LH algorithm, constrained to sample discrete points in the design space (i.e. the possible combinations), later simulated with LS-Dyna.

As described for the single modules, a double module Finite Element mesh is morphed following the same procedure. The double module configuration presents 4 geometrical variables: two for the bottom module (c_b and h_b) and two for the top module (c_t and h_t). The energy and force results of the crushing simulations are stored in an output database and later used to train the machine learning algorithms.

2.4.2 *Mechanistic feature extraction*

As we are dealing with a machine learning algorithm for the prediction of the mechanical response of structures, it is crucial to properly pre-process the data and

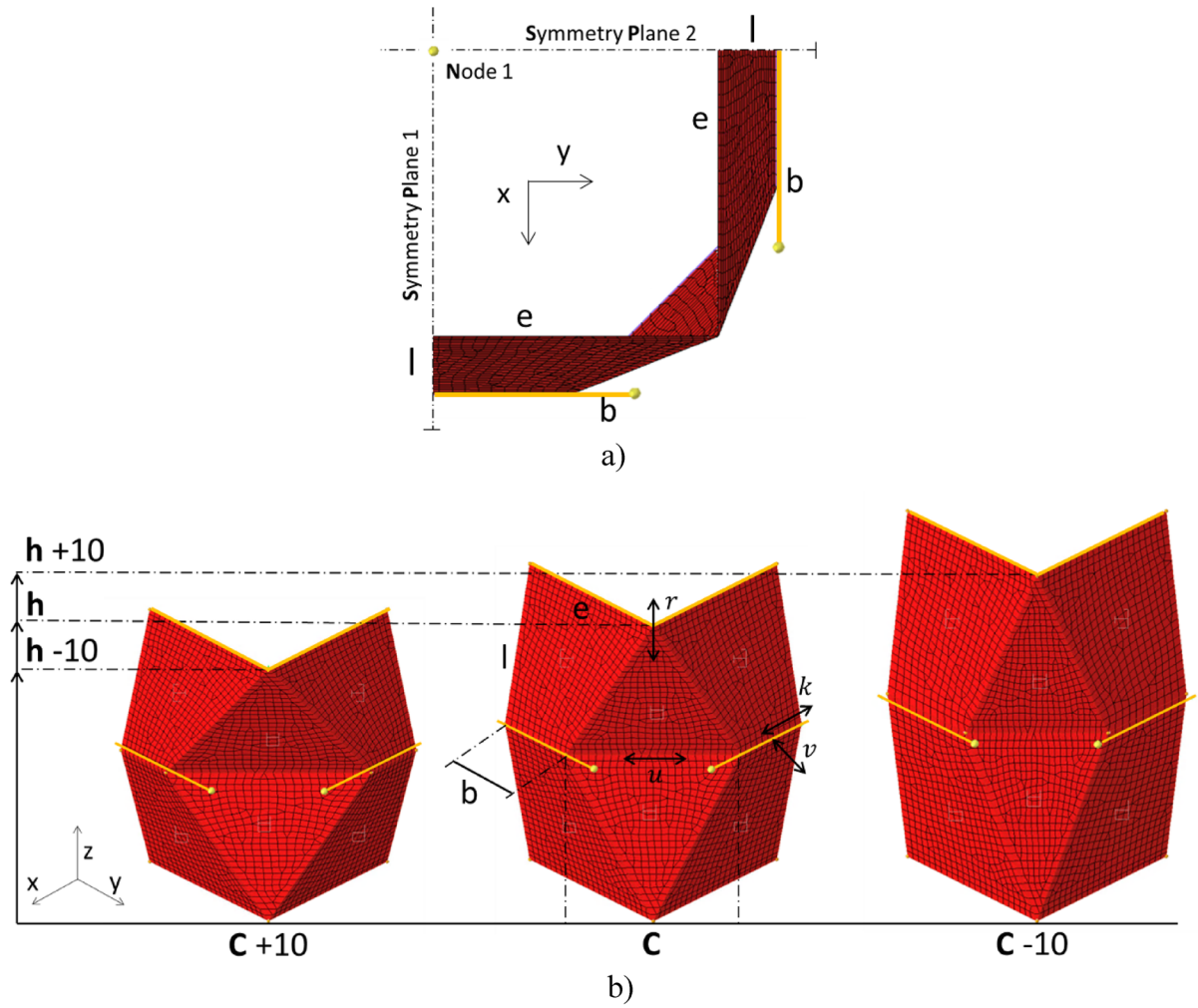

Fig. 4 Module geometry and morphing procedure description: **a** a quarter of the origami module with symmetry planes evidenced (*x*–*y* view); **b** baseline module and morphed configurations (iso view), after both c and h value modification.

extract the most relevant features influencing the final response.

Most machine learning regression algorithms take as input fixed shape variables, defining a mapping from two domains of fixed dimensions. However, the crushing response (e.g., energy vs displacement, force vs displacement) of the origami structures varies with the total height of the crushed tube. To get a consistent dimension of the curves, the displacement vectors have been normalized to their maximum value and the curves have been sampled with N linearly spaced points. Following this procedure, every input simulation is described by force and energy vectors of dimension N. Accordingly, the curves of the two single modules composing the bi-module crash tube have been concatenated into vectors of dimension 2N, following the bi-normalization transformation in Eq. (2).

$$d_{norm} = \begin{cases} \frac{d}{h_{top}} & \text{if } d < h_{top} \\ 1 + \frac{d - h_{top}}{h_{bot}} & \text{if } d > h_{top} \end{cases} \tag{2}$$

The arrangement of single-module responses into a single input vector should reflect the observed interaction of modules during the multi-module structure crush.

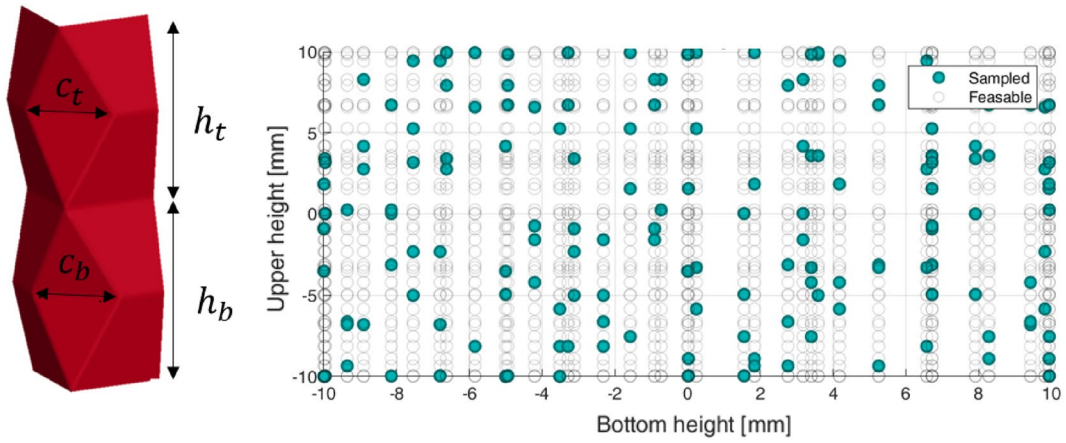

Fig. 5 Discrete LH sampling of double module geometric feature.

The NN maps the single module responses into a double-module response, from $\mathbb{R}^N$ to $\mathbb{R}^{2N}$, defining nested connections between the components of the vectors (i.e., the response of the tubes at different crushing levels). To let the NN define a consistent relation between the response of the single modules and their influence on the response of the full structure, the input vector is properly built to fix the position of the transition point from the top to the bottom module. Moreover, the two curves of the single module crushing are combined to reflect the mechanical behaviour of the assembled structures, where the crushing takes place gradually, starting from the failure of the top module followed by the crush of the bottom one.

An example of the input curve obtained with the described method is shown in Fig. 6

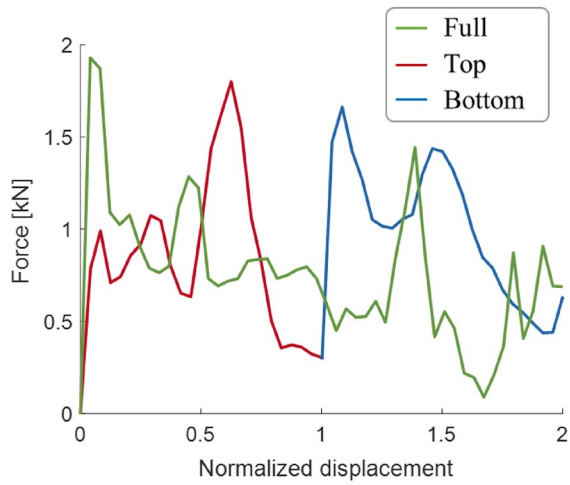

Fig. 6 In green, the output curve computed from the crashing response of the assembled structures. In red and blu, the curves obtained from the crashing of the single modules elaborated to feed the NN

2.4.3 Feed-forward neural network (FFNN)

Supervised FFNNs are traditionally trained with a set of input and output observations that the network will relate through a general operator $\mathbb{N}(\boldsymbol{w}, \boldsymbol{b})$, where trainable parameters w and b are the weights and biases of the network, respectively. A standard FFNN is composed of N layers and each layer has n neurons: fully connected networks perform the following core operation in each node:

$$y = A\left(\sum w_i x_i + b\right) \tag{3}$$

where y is the predicted value, x_i are either the input parameter of the network or the output of the previous layer, whether it is an input layer or a hidden layer (layer connected neither to input nor output); b is the bias of the neuron and $\mathcal{A}(\bullet)$ is the activation function. Parameters $\boldsymbol{w}$ and $\boldsymbol{b}$ are the trainable parameters, while the number of neurons, number of layers and activation functions are the hyper parameters of the model.

The network is optimized with a stochastic gradient descent method (Kingma & Ba 2014) and the

trainable parameters are upgraded with a back-propagation procedure, to minimize the defined loss function. The backpropagation is perpetuated iteratively in each epoch over a subset of data defined as a batch; the number of training epochs can be defined a priori or automatically defined by a stopping rule (i.e., early stopping). The loss function for the regression task is typically defined as the mean square error (MSE).

2.4.4 Physic-informed neural network

The method here proposed uses a novel PINN architecture tailored for the prediction of the axial crash response of assembled structures by embedding the equilibrium equation and energy conservation principles in the training stage. The PINN architecture (Fig. 3), is composed of a pre-processing block that performs a bi-normalization of the substructures crash response following Eq. 2. The normalized and concatenated response is passed to the hidden layers of the PINN that predict the crashing force of the origami tube. From the predicted force, the predicted absorbed energy is computed as the integral of the force over the displacement:

$$E_{comp} = \int_0^{h_i} F(x)dx. \tag{4}$$

This computation is performed inside a custom layer that takes as inputs the original displacement vector, before the normalization, and the predicted force to estimate the crashing energy.

The model is trained with a regularised loss function defined as:

$$L = \frac{1}{N}\sum\left(F_i^{pred} - F_i^{fem}\right)^2 + \alpha \cdot \sum\left(\int_0^{h_i} F^{pred}dx - E_i^{fem}\right) - \beta \cdot \frac{\sum_i \ll E_{i+1}^{pred} - E_i^{pred} \gg}{N}, \tag{5}$$

where F_i^{fem} and F_i^{pred} are the FEM computed and PINN predicted values of the crashing force at the ith frame, being N the total number of frames; h_i is the crashing displacement at the ith frame and E_i the computed energy.

The first term of Eq. (5) penalises the prediction errors on the force, while the second and third penalise the physical inconsistency of the predictions with the energy conservation criteria. Indeed, a discrepancy of the computed energy with the value computed with the FEM yield an increase in the second term of loss function proportional to the hyperparameter α, guiding the optimization through physically-consistent results. The parameters α and β are non-negative scalars that weigh the influence of the physics-related terms on the total loss, scaling it to the same order of magnitude as the other contributions. In the last term of Eq. (5), the operator $<<\bullet>>$ gives one if the argument is positive and zero otherwise, penalizing the predictions with a decreasing trend of the absorbed energy. The weights α and β have been set equal to 0.1 and 1, respectively, to achieve consistent orders of magnitude of the different terms.

3 Results and discussion

In this section, the results of the surrogate modelling approach for the design of the origami crash tube are presented. First, the FFNN and PINN are trained on the available results of FEA, and then the crash response predicted with the NN models is compared with the reference curves from the FEM to assess the accuracy of the method and compare the FFNN with the PINN. Finally, the PINN is used to optimize the geometry of the origami tube and the prediction of the response of the optimized geometries is validated with the FE model.

3.1 Double module crash prediction

The architecture of the FFNN has been optimized based on the sensitivity analysis carried out on the model accuracy: the number of layers and the number of neurons per layer have been varied to identify the best architecture to be used. Figure 7 reports the value of the loss function after 500 epochs for different architectures: Fig. 7b indicates that deep networks lead to low accuracy due to the increase of the network hyper parameters that compromise the convergence of the training; Fig. 7a shows a small increase in the loss with the increasing width of the network.

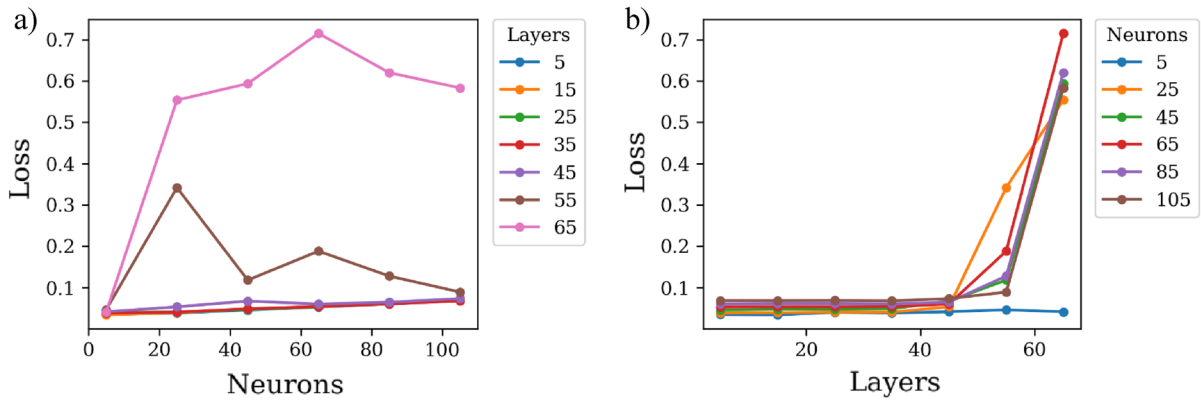

Fig. 7 The value of the loss function at the end of the training of the FFNN with different number of neurons per layer (**a**) and number of layers (**b**).

Table 2 Summary of FFNN optimized structures with activation function and number of neurons of each layer

Layer	Neurons	Activation	Output shape
Input	2N	Linear	(2N, 1)
Dense 1	15	ReLU	(20, 1)
Dense 2	15	ReLU	(20, 1)
Dense 3	15	ReLU	(20, 1)
Dense 4	15	ReLU	(20, 1)
Dense 5	15	ReLU	(20, 1)
Output	2N	Linear	(2N, 1)

As a conclusion of this analysis, short and narrow architecture is suggested.

On the base of the results of the sensitivity analysis, the FFNN architecture is made of 5 stacked layers with 15 neurons each. Further performed analysis suggested that the network accuracy is independent of the activation function used in the hidden layers for the case of Rectified Linear Unit (ReLU), SELU and tanh, leading to the adoption of the ReLU due to its higher computational efficiency. The same architecture has been used for the PINN.

The activation function of the input and output layers is linear so that the output of the last layer is not biased by the activation function. The layered architecture of the FFNN is summarized in Table 2.

The FFNN was trained with 80% of the available data, while the remaining 20% was used as a validation dataset to check the eventual overfitting of training data. The weights and bias of the NN were updated through a back-propagation algorithm by minimizing the Mean Square Error loss function of Eq. (4). The adaptive moment estimation optimizer algorithm Adam (Kingma & Ba 2014) has been adopted.

As previously described, the PINN takes as input the force response, the energy response, and the original displacement vector before normalization, which is used to compute absorbed energy from the predicted force. The displacement is not computed by a trainable layer and thus does not increase the number of hyper parameters of the NN.

The values of the loss terms for the FFNN and PINN are compared in Fig. 8. The FFNN archives smaller overall errors in the prediction of the force response while struggling in converging to an accurate prediction of the energy. As a result, the FFNN shows a 10% lower RMSE for the force, while the PINN performs better in the prediction of the absorbed energy with an approximately 70% lower RMSE.

The training curve of the PINN is reported in Fig. 9, to highlight the simultaneous convergence of the prediction towards accurate and yet physically compliant curves. Indeed, the values of the loss term associated with the PINN accuracy in predicting the force response are correlated with the loss curve of the energy balance term confirming that the interplay of such terms improves the training of the network.

The coupling of the force and energy prediction in the PINN limits the solution space of the Networks

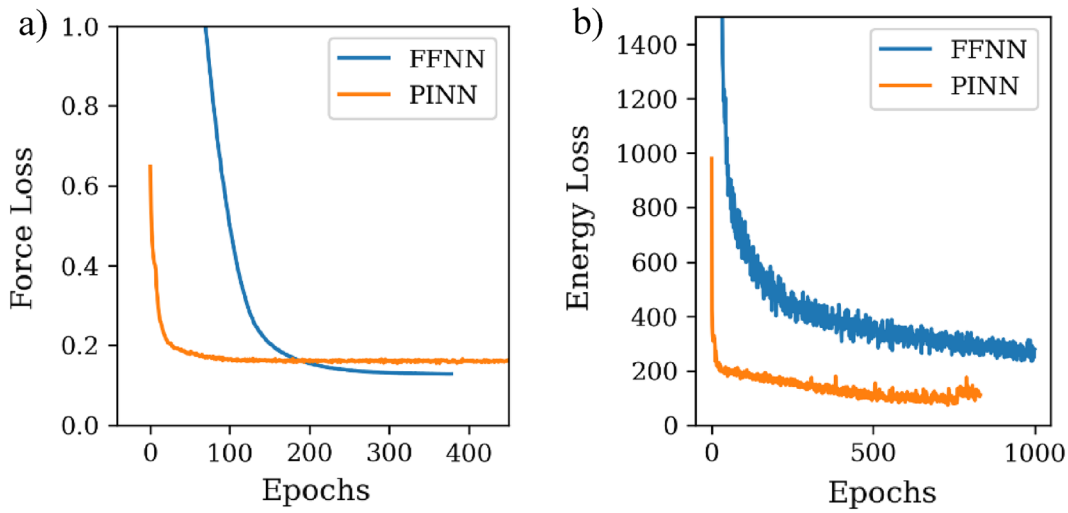

Fig. 8 The loss values for the predicted force **a** and absorbed energy **b** during the training of the FFNN and PINN

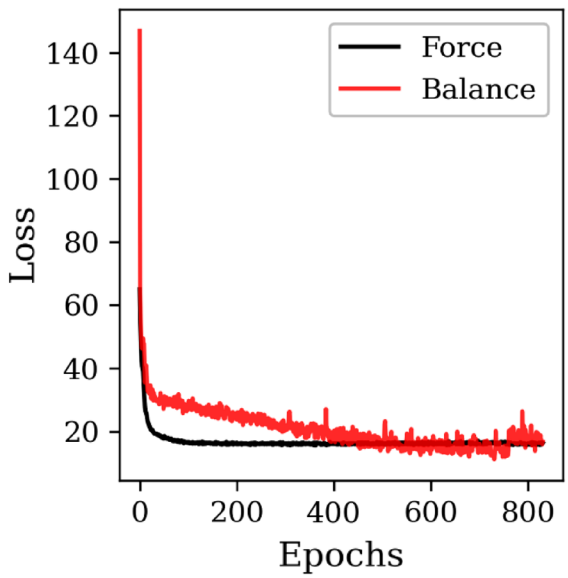

Fig. 9 The values of the force and balance terms in the loss function of the PINN during the training

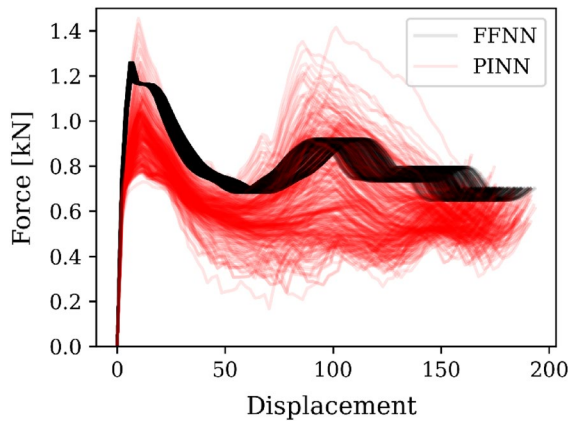

Fig. 10 The force response predicted with the FFNN and the PINN for all the crash box configurations in the training dataset

that reflects in higher RMSE for the force prediction but yields a physic-compliant energy response. However, even if the values of the loss functions give an overall indication of the accuracy of the method, in the case of complex datasets with high variability, lower RMSE could be consequent to an input-insensitive network that outputs an average value regardless of the input data. Indeed, in the FFNN, the predicted force response is insensitive to the input configurations, while this is prevented in PINN by coupling the energy and force response with the physic layer, as shown in Fig. 10.

The curves precited with the FFNN and PINN for all the crash box configurations in the training dataset are compared in Fig. 10. The high variability of the force curves predicted by the PINN is in line with what observed from the FEM in (Ciampaglia et al. 2020a, b), while the FFNN predicts the same curve for every configuration (scaled back to the original displacement in the figure), being insensitive to the

crash box geometry and ultimately losing any predictive capability.

This confirms that the analysis of the results of ML methods applied to engineering problems should not be limited to the prediction errors described by the common data science metrics (e.g., MSE, RMSE, …), but an extended analysis is needed to assess the usability of such methods for engineering problems.

Figure 10 highlights that the response of the assembled crash box in the initial stage of the crashing has a defined trend, with a first peak and a following valley, which values are mostly influenced by the top module geometry. While the force curve in the second stage of the crash, after the first module is completely crashed and the load is transferred to the lower part of the origami tube, has a variable trend governed by self-contact and complex failure phenomena leading to different average force and consequently absorbed energies.

Figure 11 reports the crushing response of an origami crash tube with lobe widths equal to 47 mm and 38 mm and a height of 78.5 mm and 84.5 mm, for the bottom and top modules, respectively. The result of the FEM model is compared with the prediction of the PINN and FFNN, both in terms of force and absorbed energy. The diagram of Fig. 5a shows that in this specific case, the PINN model can predict the crush response with a 15% error on the peak load and an 8% error on the average force, while the FFNN shows a 34% error on the peak force and 7% error on the average. However, the FFNN is constant throughout the dataset, making its predictions ineffective for the design of the crash box.

The diagram of Fig. 11b puts evidence that the values of the absorbed energy during the crash stroke predicted by the PINN model are very close to those resulting from the FE simulation, while those predicted by the FFNN model are largely below those resulting from the FE simulation. Therefore it can be concluded that the proposed PINN method is preferable to the FFNN, at least for this type of analysis.

Figure 12 analyses the results of the PINN at different crushing stages compared with the reference values from the FEM. It can be observed that the predicted energy has a larger error in the first stage of the crushing, due to the struggle of the model in accurately predicting the first peak force, while it converges around an average value of 0.1 after that 20% of the origami crash box is crashed. On the other hand, it should be noted that the FE predicted value of the force at the collapse initialization (first peak) has high uncertainty and suffers the larger oscillation of the FEM results that are overall smoothed and averaged by the PINN that predicts smoother curves, resulting in larger errors with the increasing crushing. However, the average error is almost constant toward the crashing, with higher values (between 0.2 and 0.3) in correspondence to the crashing of the second modulus where non-linear and history-dependent

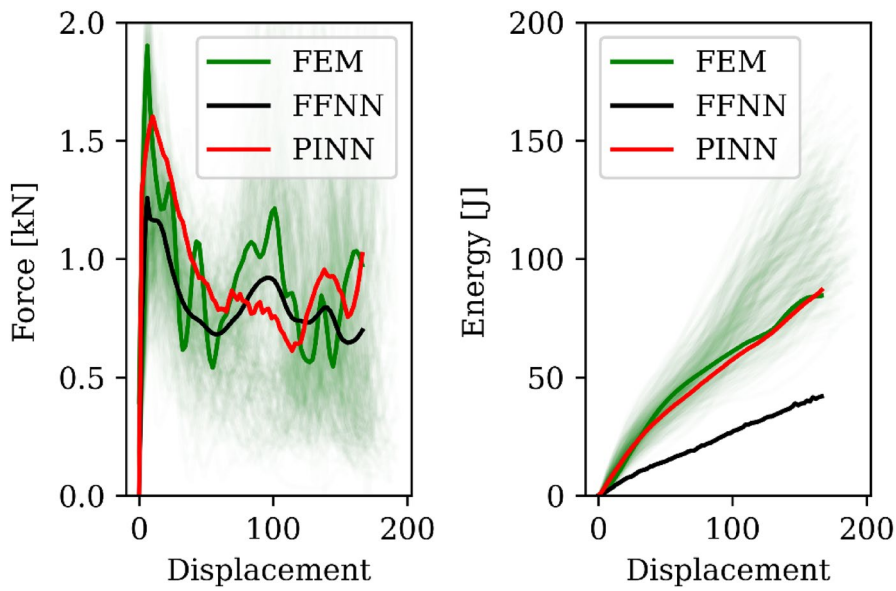

Fig. 11 The force **a** and absorbed energy **b** predictions of the PINN and FFNN on a validation combination excluded from the training dataset (shaded curves) compared with FEM simulation (solid curve). The origami crash box has $h_{bot} = 78.5$, $h_{top} = 84.5$, $c_{bot} = 47$, $c_{top} = 38.5$

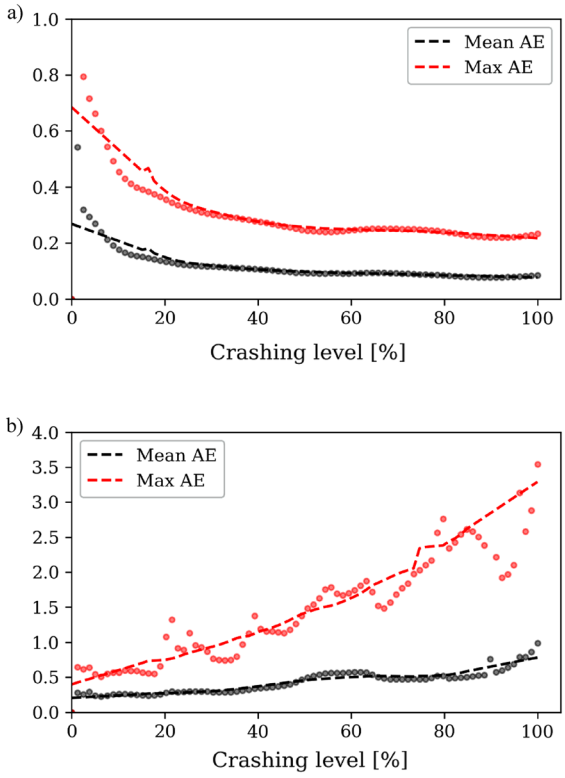

Fig. 12 The mean and maximum Absolute Error (AE) of the PINN predictions for the absorbed energy (**a**) and force (**b**) predictions at different level crashing. Each point is the average of all the training errors, while the dashed lines represent an interpolation of the points

phenomena take place and negatively affect the predictive capability of the model.

3.2 Optimization of the origami tube with the PINN

The PINN model is used to optimize the geometry of the origami-shaped crash box by initially simulating 40 single modules (N = 40) with different geometry. The full domain that the PINN can explore counts 1560 different configurations that can be predicted with the proposed algorithm. The energy response results are reported in Fig. 13: the rapid exploration of the extended DoE confirms that the variation of origami geometry, even not affecting the total mass of the component, leads to a significant variation in the absorbed energy as observed in (Ciampaglia et al. 2020a, b). All the possible configurations of the 40 modules have been predicted with the PINN and are reported in Fig. 13.

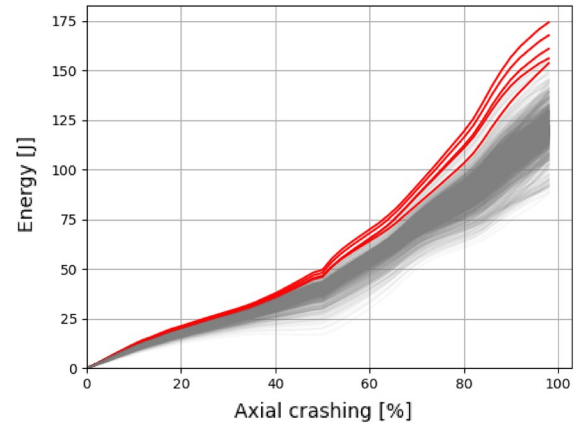

Fig. 13 Machine learning predictions of 1560 different geometric configurations of a double module origami-inspired crash box, in red the five curves with the highest absorbed energy

Figure 12 showed that the accuracy of the PINN in predicting the energy values varies within different crashing intervals, with more accurate prediction in the initial region, gradually decreasing until the complete crashing where a high non-linear failure mechanism combines. Considering this, a scoring method is introduced to evaluate the best curves by ranking all predicted responses at different intervals and assigning a score (5 to the best prediction and 0 to the worst prediction) to the best five predictions at each crashing level (Fig. 14).

The proposed scoring strategy counters the accuracy decrease in the prediction of the absorbed energy close to the complete crushing, rewarding the crash tubes that show a consistently higher performance among all the configurations. Indeed, Fig. 14 shows the normalized energy absorption of all predicted configurations at 40, 70 and 90% of ultimate displacement, evidencing the existence of temporary peaks vanishing outside certain intervals. This is in line with the energy curves shown in Fig. 13, where a small difference in the absorbed energy is evidenced for the first phase of the crashing where the curves are grouped. With the increasing displacement, the absorbed energy of the different origami tubes diverges from the average values, yielding the presence of optimal configurations with higher energy absorption capability. These reflect the yellow spots in the response map at 90% of the crashing in Fig. 15.

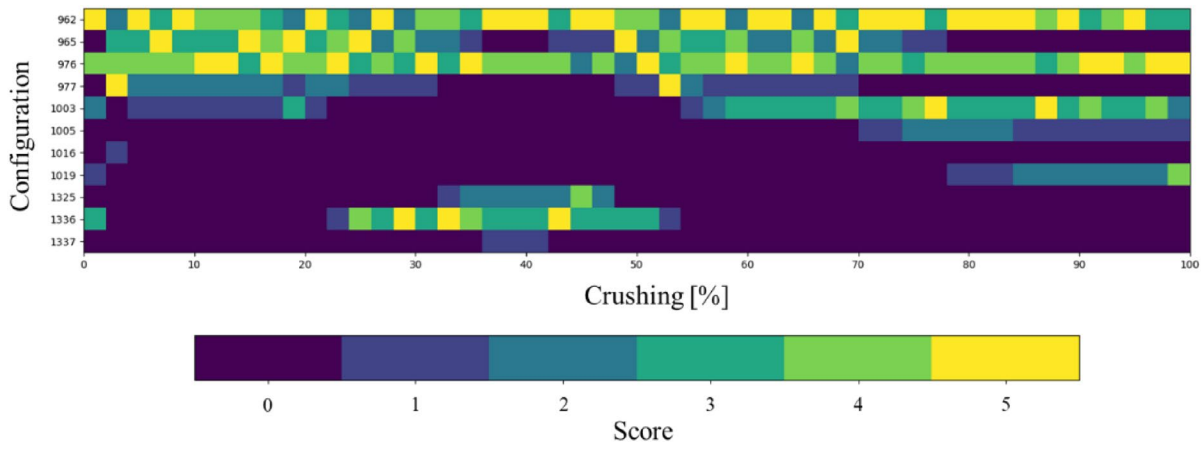

Fig. 14 Scoring algorithm ranking a selection of the best different configurations at each crashing level by the normalized absorbed energy. Scores from 1 to 5 are assigned at each interval

Fig. 15 Heatmap of the normalized absorbed energy at 40%, 70% and 90% crashing intervals

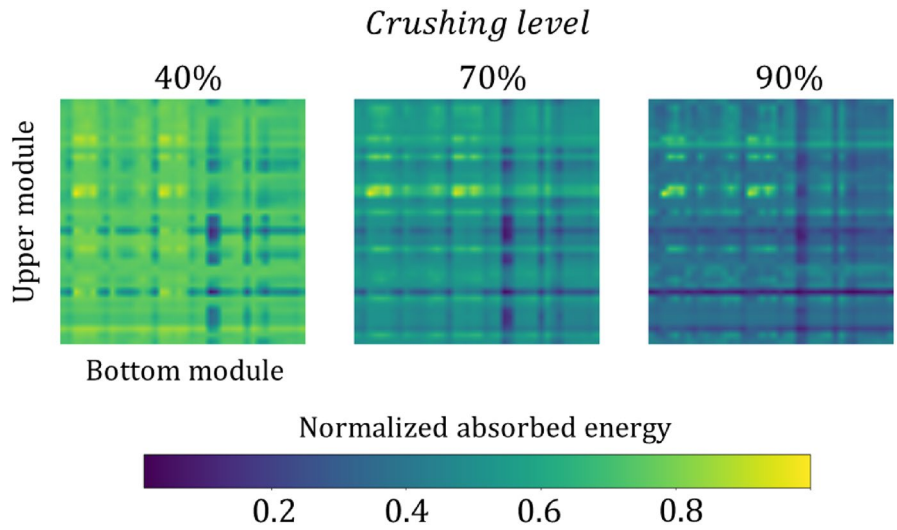

The best two configurations show (see Fig. 16) a total absorbed energy of 175 and 171 J, respectively, with their geometrical features reported in Table 3.

The crash response for these origami tubes is then computed using the FE model and the results are compared in terms of absorbed energy, to confirm the quality of the results and the efficiency of the machine learning-based optimization algorithm.

The comparison is reported in Fig. 16 and shows a good agreement between the response predicted by the PINN algorithm and that calculated through the FE analysis up to 80% of the total crashing. This proves that the proposed methodology can be reliably applied to the design of the origami tube and guarantees a remarkable reduction of the computational effort.

The presented PINN algorithm can predict the crashing response of the assembled structures with reduced computational efforts and an overall good accuracy; more specifically, given a set of N single module crash simulations, the algorithm can estimate the response of N!/(N-2)! geometric configurations of the double modules crash box by drastically reducing the computational cost. Indeed, once the model is trained, the assessment of the full crash box response computed with the PINN takes approximately 0.1 s

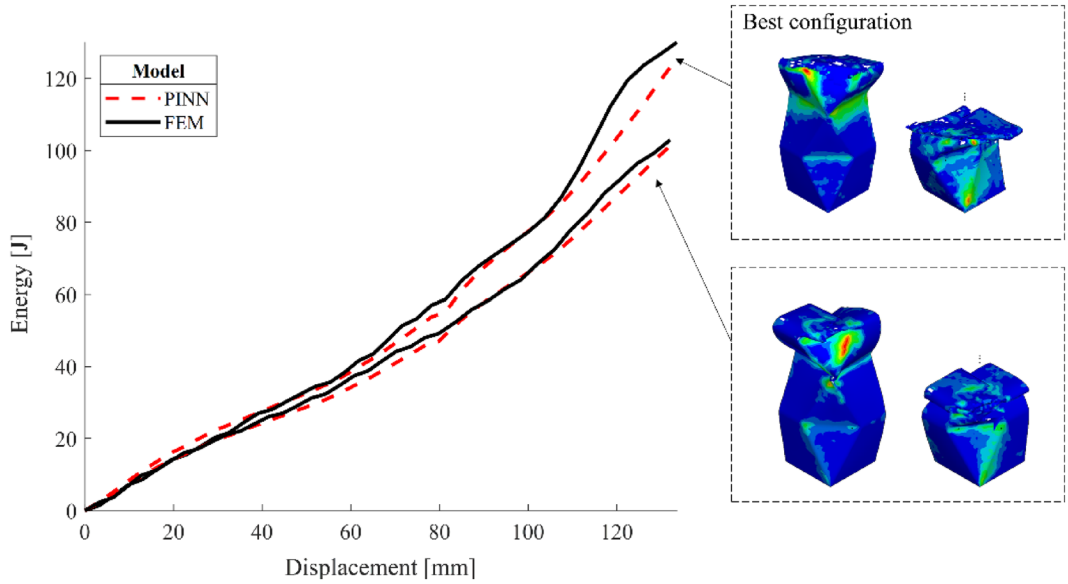

Fig. 16 The absorbed crash energy of the optimized configurations predicted with the PINN model compared with the results of the FEM

Table 3 Geometrical features of the two configurations with the highest absorbed energy predicted by the PINN

	c_bot [mm]	c_top [mm]	h_bot [mm]	h_top [mm]	E [J]
1	42.2	54.5	93.25	81.4	175
2	42.2	41.2	63.2	79.8	171

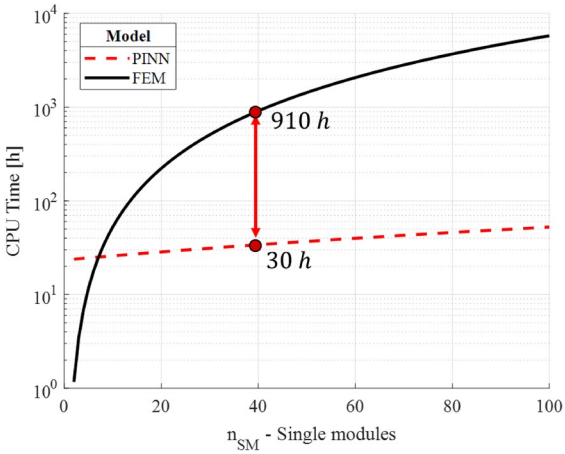

Fig. 17 Computational time comparison between FEM and ANN optimization

on a 16 CPU laptop, while an FEA of a crash box with two modules takes around 35 min on a 40 CPU cluster. Figure 17 shows the computational saving in terms of simulation hours for different N, showing an average speed-up of 30 times.

The computational cost of the PINN is mostly affected by the simulation time (i.e., 98% of total time) required to build the training database. More efficient numerical methods (Vu-Bac et al. 2018) would reduce the simulation time of the tube crashing and enhance the efficiency of the proposed approach.

3.3 Discussion

In terms of model architecture, the optimization efforts led to a concise FFNN design with 5 layers, each containing 15 neurons. Interestingly, the choice of activation function in hidden layers had limited influence on performance, with ReLU's computational efficiency making it the preferred option. This architecture proved equally effective for the PINN, ensuring consistency between models.

When comparing predictive accuracy between the FFNN and PINN, it's evident that the FFNN holds a slight advantage with a 10% lower RMSE in force prediction. However, the FFNN struggles in

accurately forecasting energy responses. In contrast, the PINN demonstrates approximately 70% lower RMSE in absorbed energy prediction, highlighting its superiority in capturing energy-related phenomena. Notably, the PINN's unique capacity to ensure physically compliant results through the coupling of force and energy predictions sets it apart.

A key takeaway from this analysis is the importance of evaluating ML models for input sensitivity, beyond traditional metrics like MSE and RMSE. The FFNN's insensitivity to variations in crash box geometry, resulting in identical predictions for all configurations, underscores this point. The PINN, by accounting for these variations, introduces a higher degree of variability in force predictions, aligning more closely with real-world observations from Finite Element Analysis (FEM).

The results unveil the dynamic nature of crash responses, with distinct trends observed at different stages of the crash. Initial force is predominantly influenced by the origami top module's geometry, while later stages involve intricate phenomena governing force and energy absorption.

The PINN's practicality extends beyond predictive accuracy; it proves instrumental in optimizing origami tube geometry. Extensive simulations of 40 single modules with diverse geometries, evaluating 1560 different configurations, highlight the impact of even minor geometry adjustments on energy absorption. The proposed scoring strategy effectively identifies superior configurations, emphasizing the existence of geometries with enhanced energy absorption capabilities.

One of the standout achievements of the PINN approach is its remarkable reduction of computational effort. Swift estimation of responses for numerous geometric configurations of double module crash boxes, providing results within seconds on standard hardware, stands in stark contrast to the hours required by Finite Element Analysis (FEA) on high-performance clusters.

4 Conclusion

Optimizing structures subjected to crush presents inherent complexities, as improving energy absorption requires an intensive design phase that can demand significant computational resources. However, this optimization plays a pivotal role in enhancing the safety of vehicle occupants by improving the energy-absorption capabilities of such structures.

In this study, novel Physics-informed Neural Networks (PINN) approach to address the complexities of origami-shaped crash tube optimization and design has been developed. The research demonstrates the potential of PINN as an efficient and reliable surrogate modelling technique for predicting energy absorption response of a crush tube while reducing the computational demands associated with traditional optimization methods. Indeed, common optimization methods rely on structural simulations that are computationally highly demanding and are generally surrogated by model that requires abundant data to achieve sufficient accuracy. To address the need of a computationally efficient, yet accurate, surrogate model of the tube crashing, a physics-informed neural network has been developed that predicts the energy absorbed by an origami shaped tubes made of composite. The origami structure is composed of two vertically stacked sub-structures, named moduli, that present a bottom and top squared section with an octagonal profile in the centre. The geometrical parameters of the octagonal shape and the height of the moduli is optimized to maximize the energy absorption while limiting the force peaks, aiming to preserve the occupants from dangerous accelerations and stick with the passive safety requirements.

The accuracy of standard surrogate modelling techniques depends solely on the amount of data available, which severely limits their efficiency. To overcome this problem, a NN scheme based on the physical knowledge of the problem (PINN) has been adopted in this work, thus developing an innovative methodology. The goal was to correlate the crushing response of individual modules to that of the entire origami tube. The training of the PINN was performed on a dataset generated through finite element simulations, previously validated on experimental results. The results showed that the PINN can correctly predict the crushing response of the origami crash tube, while remarkably reducing the computational cost, thus avoiding the extensive exploration of the design domain through Finite Element simulation campaigns. The comparison with a standard surrogate modelling technique, showed the superior accuracy of the PINN scheme for the same amount of available

data. Indeed, the mean square error of the PINN is below 15%, except in the initial stage concerning the initial peak force, while that of the FFNN algorithm was almost equal to 20%.

Finally, the PINN has been used to optimize the geometry of the origami tube with the goal of maximizing the absorbed energy. The results of the two best-performing structures have been compared to those obtained through finite element analysis, showing a good agreement of the predicted energy-displacement curves with the finite element results, validating the reliability of the PINN for the design of the origami crash tube. The proposed approach consistently reduces the computational effort with respect to a standard optimization based on FEM, with the PINN requiring 30 h to complete the job, while almost 910 h are necessary to simulate all the retained configurations of the origami tube. Further reduction of the computational cost could be achieved using more efficient numerical models for the generation of the database.

Funding Open access funding provided by Politecnico di Torino within the CRUI-CARE Agreement.

Data availability The datasets generated during and/or analysed during the current study are available from the corresponding author on reasonable request.

References

ASTM Standard D3410/D3410M-16, 2021, Standard Test Method for Compressive Properties of Polymer Matrix Composite Materials with Unsupported Gage Section by Shear Loading. ASTM International, West Conshohocken, PA (2021). https://doi.org/10.1520/D3410/D3410M-16, https://www.astm.org

Avalle, M., Chiandussi, G., & Belingardi, G. (n.d.). *Design optimization by response surface methodology: application to crashworthiness design of vehicle structures*. https://doi.org/10.1007/s00158-002-0243-x

Baler, H.: Ill-posed problems in structural optimization and their practical consequences In Structural Optimization. Springer, Berlin (1994)

Boreanaz, M., Belingardi, G., Maia, C.D.F.: Application of the origami shape in the development of automotive crash box. Mater Des Process Commun **2**(4), e181 (2020). https://doi.org/10.1002/MDP2.181

Boria, S., Scattina, A., Belingardi, G.: Axial energy absorption of CFRP truncated cones. Compos. Struct. **130**, 18–28 (2015). https://doi.org/10.1016/J.COMPSTRUCT.2015.04.026

Boria, S., Scattina, A., Belingardi, G.: Experimental evaluation of a fully recyclable thermoplastic composite. Compos. Struct. **140**, 21–35 (2016). https://doi.org/10.1016/J.COMPSTRUCT.2015.12.049

Boria, S., Belingardi, G., Fiumarella, D., Scattina, A.: Experimental crushing analysis of thermoplastic and hybrid composites. Compos. Struct. **226**(February), 111241 (2019). https://doi.org/10.1016/j.compstruct.2019.111241

Ciampaglia, A., Fiumarella, D., Boursier Niutta, C., Ciardiello, R., Belingardi, G.: Impact response of an origami-shaped composite crashbox: experimental analysis and numerical optimization. Compos. Struct. **256**, 113093 (2020a). https://doi.org/10.1016/j.compstruct.2020.113093

Ciampaglia, A., Santini, A., Belingardi, G.: Design and analysis of automotive lightweight materials suspension based on finite element analysis. J Mech Eng Sci (2020). https://doi.org/10.1177/0954406220947457

Dias, J. P., Cadete, R. N., & Pereira, M. S. (2005). Optimization in vehicle crashworthiness design using surrogate models COST TU1101 View project 6 th World Congresses of Structural and Multidisciplinary Optimization Optimization in vehicle crashworthiness design using surrogate models. https://www.researchgate.net/publication/250092920

Fiumarella, D., & Raponi, E. (2020). *Experimental analysis and numerical optimization of a thermoplastic composite in crashworthiness*.

Hadamard, J.: Sur les problèmes aux dérivées partielles et leur signification physique. Princeton Univ. Bull. **13**, 49–52 (1902)

Hallquist, J. O. (2006). *LS-DYNA ® THEORY MANUAL*. www.lstc.com

Hou, S., Li, Q., Long, S., Yang, X., Li, W.: Design optimization of regular hexagonal thin-walled columns with crashworthiness criteria. Finite Elem. Anal. Des. **43**(6–7), 555–565 (2007). https://doi.org/10.1016/J.FINEL.2006.12.008

ASTM Standard 5379/D5379M – 19, 2021, Standard Test Uethod for Shear Properties of Composite Materials by the V-Notched Beam Method. ASTM International, West Conshohocken, PA (2021). https://doi.org/10.1520/D5379_D5379M-19E01, https://www.astm.org

Kingma, D. P., & Ba, J. L. (2014). Adam: A Method for Stochastic Optimization. *3rd International Conference on Learning Representations, ICLR 2015 - Conference Track Proceedings*. https://doi.org/10.48550/arxiv.1412.6980

Koronis, G., Silva, A., Fontul, M.: Green composites: a review of adequate materials for automotive applications. Compos. B Eng. **44**(1), 120–127 (2013). https://doi.org/10.1016/J.COMPOSITESB.2012.07.004

Li, Y., You, Z.: Origami concave tubes for energy absorption. Int. J. Solids Struct. **169**, 21–40 (2019). https://doi.org/10.1016/J.IJSOLSTR.2019.03.026

Ma, J., Chai, S., Chen, Y.: Geometric design, deformation mode, and energy absorption of patterned thin-walled structures. Mech. Mater. **168**, 104269 (2022). https://doi.org/10.1016/J.MECHMAT.2022.104269

Ma, J., & You, Z. (2014). A Novel Origami Crash Box With Varying Profiles. *Proceedings of the ASME Design Engineering Technical Conference*, *6 B*. https://doi.org/10.1115/DETC2013-13495

Martulli, L.M., Creemers, T., Schöberl, E., Hale, N., Kerschbaum, M., Lomov, S.V., Swolfs, Y.: A thick-walled sheet moulding compound automotive component: Manufacturing and performance. Compos Part A Appl Sci Manufact **128**(2019), 105688 (2020). https://doi.org/10.1016/j.compositesa.2019.105688

Nemeth, I. (n.d.). *Standard Test Method for Tensile Properties of Polymer Matrix Composite Materials*.

Raissi, M., Perdikaris, P., Karniadakis, G.E.: Physics-informed neural networks: A deep learning framework for solving forward and inverse problems involving nonlinear partial differential equations. J. Comput. Phys. **378**, 686–707 (2019). https://doi.org/10.1016/J.JCP.2018.10.045

Raponi, E., Fiumarella, D., Boria, S., Scattina, A., Belingardi, G.: Methodology for parameter identification on a thermoplastic composite crash absorber by the sequential response surface method and efficient global optimization. Compos. Struct. **278**(July), 114646 (2021). https://doi.org/10.1016/j.compstruct.2021.114646

Rwawiire, S., Tomkova, B., Militky, J., Jabbar, A., Kale, B.M.: Development of a biocomposite based on green epoxy polymer and natural cellulose fabric (bark cloth) for automotive instrument panel applications. Compos. B Eng. **81**, 149–157 (2015). https://doi.org/10.1016/J.COMPOSITESB.2015.06.021

Sakaridis, E., Karathanasopoulos, N., Mohr, D.: Machine-learning based prediction of crash response of tubular structures. Int. J. Impact Eng **166**, 104240 (2022). https://doi.org/10.1016/J.IJIMPENG.2022.104240

Samaniego, E., Anitescu, C., Goswami, S., Nguyen-Thanh, V.M., Guo, H., Hamdia, K., Zhuang, X., Rabczuk, T.: An energy approach to the solution of partial differential equations in computational mechanics via machine learning: Concepts, implementation and applications. Comput. Methods Appl. Mech. Eng. **362**, 112790 (2020). https://doi.org/10.1016/J.CMA.2019.112790

Vu-Bac, N., Duong, T.X., Lahmer, T., Zhuang, X., Sauer, R.A., Park, H.S., Rabczuk, T.: A NURBS-based inverse analysis for reconstruction of nonlinear deformations of thin shell structures. Comput. Methods Appl. Mech. Eng. **331**, 427–455 (2018). https://doi.org/10.1016/J.CMA.2017.09.034

Wu, J., Zhang, Y., Li, K., Su, L.: Origami-inspired metamaterials hierarchical structure with tailorable crushing behavior. Constr. Build. Mater. **345**, 128328 (2022). https://doi.org/10.1016/J.CONBUILDMAT.2022.128328

Ye, H., Ma, J., Zhou, X., Wang, H., You, Z.: Energy absorption behaviors of pre-folded composite tubes with the full-diamond origami patterns. Compos. Struct. **221**, 110904 (2019). https://doi.org/10.1016/J.COMPSTRUCT.2019.110904

Ye, H., Zhou, X., Ma, J., Wang, H., You, Z.: Axial crushing behaviors of composite pre-folded tubes made of KFRP/CFRP hybrid laminates. Thin-Walled Structures **149**, 106649 (2020). https://doi.org/10.1016/J.TWS.2020.106649

Zhang, P., Sun, Z., Wang, H., Xiang, X.: Performance study of origami crash tubes based on energy dissipation history. Energies (2022). https://doi.org/10.3390/en15093109

Zhao, X., Hu, Y., Hagiwara, I.: Shape optimization to improve energy absorption ability of cylindrical thin-walled origami structure. J Comput Sci Technol **5**(3), 148–162 (2011). https://doi.org/10.1299/JCST.5.148

Zhou, C., Zhou, Y., Wang, B.: Crashworthiness design for trapezoid origami crash boxes. Thin-Wall Struct **117**, 257–267 (2017). https://doi.org/10.1016/J.TWS.2017.03.022